DYNAMICAL PROPERTIES OF THE CHROMOSPHERE AND TRANSITION REGION IN THE SUPERGRANULAR NETWORK : WHAT PRECISION OF THE SPECTRAL LINE CHARACTERISTICS CAN BE REACHED ?

W. Curdt[1], A. Kučera[2], J. Rybák[2], U. Schühle[1], H. Wöhl[3]

[1]Max-Planck-Institut für Aeronomie, D-37189 Katlenburg-Lindau, Germany
[2]Astronomical Institute of the Slovak Academy of Sciences, SK-05960 Tatranská Lomnica, Slovakia
[3]Kiepenheuer-Institut für Sonnenphysik, D-79104 Freiburg, Germany

ABSTRACT

First SUMER results from our cooperative observations of the solar quiet atmosphere dynamics with the SUMER/SOHO and VTT/Tenerife instrumentation are presented. The contribution is focused at first on the possible *real* spectral, spatial and temporal resolutions which could be reached using the SUMER spectrometer measurements of the solar quiet atmosphere. Two flat-field patterns as well as different reduction methods for noise estimation and frame destretching are used for estimation of the line parameters inaccuracy caused by the instrumental effects. The overall long-term spectral line drift was found as probable consequence of the slight variations of the SUMER mechanics temperature. Finally the temporal variability of the transition region above both the supergranular internetwork and boundary is presented using the O VI 1037.61 Å and nearby C II lines with the resolution of 2 arc sec and 15 seconds showing significant temporal and spatial variations. The significant relationship of the O VI line intensity with the remarkable red-shift was found in the network boundary but this phenomenon was found not to be unambiguous.

Key words: Sun: transition region – Sun: dynamics – instrumentation: SUMER.

1. INTRODUCTION

The SUMER spectrometer (Wilhelm et al. 1996) onboard the SOHO mission has opened a new possibility to investigate the dynamics of the solar outer atmosphere from the solar upper chromosphere through transition zone to low corona. First results, presented by various teams (e.g. Wilhelm et al., 1997, Lemaire et al., 1997, Steffens et al., 1997), confirmed the expected dramatical increase of the spatial and spectral resolution of SUMER observations comparable to the previous NRL/HRTS results also for UV wavelength range below 1150 Å.

The velocity fields among other physical and structural properties have already been analyzed in order to reveal whether the low photospheric pattern takes place also in the higher photosphere, e.g. by Espagnet et al. (1995) and Kučera et al. (1995). The aim of our project is to extend the analysis of the dynamics from the photosphere to the chromosphere and transition region using the parallel spectral observations of the VTT/Tenerife and SUMER/SOHO instrumentation (see our UDP 8.1.2.66 in the SUMER Red Book). The preliminary report about the September 1996 parallel observations was already given in paper of Curdt et al. (1997) where more details regarding the VTT measurements can be found.

The present contribution is focused on the performed SUMER data reduction and the effects which were found during the handling of these data as affecting the final spectral characteristics of lines. The examples of O VI 1037.61 Å, C II 1036.337 and 1037.018 Å were used for the illustration of the detected relations and facts. The temporal behaviour of the O VI line maximal intensity and Doppler velocity is presented and discussed as well.

2. OBSERVATIONS

Generally SUMER measurements were taken in one of two sets of lines around the 1030 Å and 1310 Å, both using 6 windows 25 pixels wide (the complete list of lines is given in Curdt et al., 1997). The slit of 1 arc sec width and of the height 120 or 24 arc sec was exploited. Observations were started by the 2D area sequential scanning, at first of a larger one (38x120 arc sec), then also of its centred subarea (8 arc sec wide), in order to get images of the investigated region covering also its development. The next measurements consisted of 1D observations lasting up to 3 hours in the central position of the previous 2D scans. Finally, the observational run was finished with a burst sequence of short exposures taken in the same 1D position until the available onboard memory was filled. The integration times from 15 seconds (large scans, long 1D sequence) down to 2.5 seconds (burst exposures) were selected as the compromise between the required temporal resolution and the available telemetry rate and the detector efficiency. The compensa-

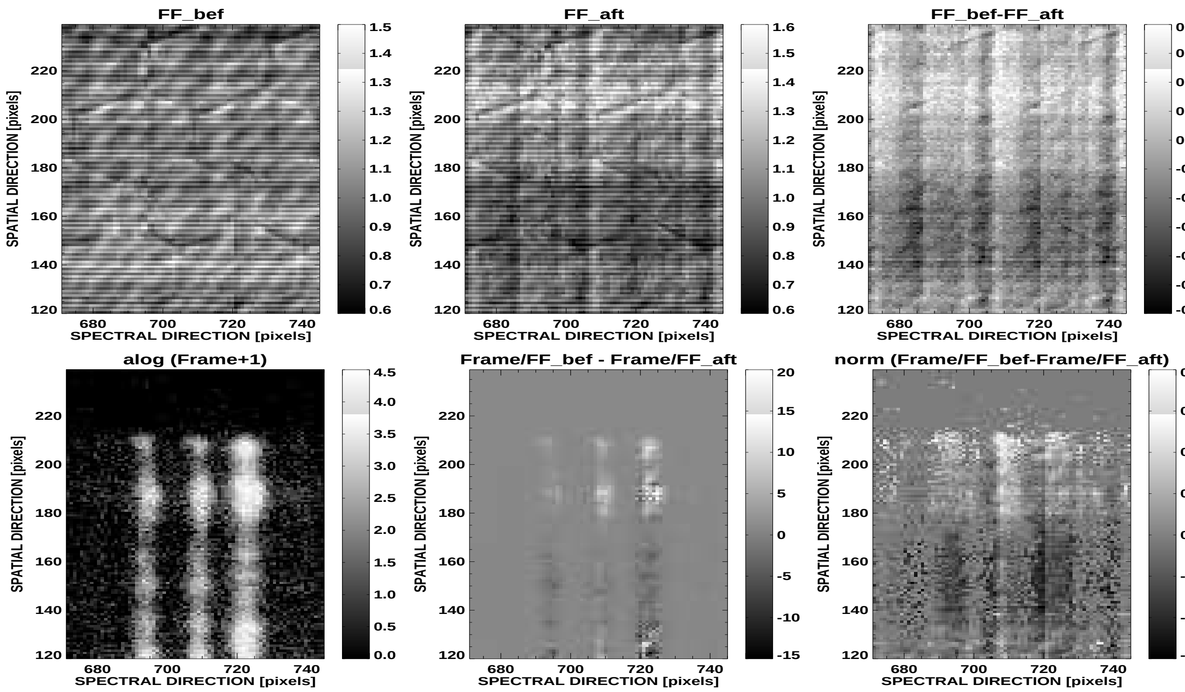

Figure 1. The particular area of normalized flat-field frames, taken before and after our measurements, and their difference are displayed in the upper panels of the figure. The application of these information on the selected spectral frame is illustrated in the bottom panels together with the normalized differences of this spectral frame reduced for both flat-fields (right panel).

tion of the solar rotation was applied during the whole observational run keeping the initial solar disk center as the target. No binning of the acquired data was applied onboard but the quasilog compression scheme was selected to speed up the telemetry of the acquired data.

This contribution is based on measurements of Sept. 7, 1996 when the Lyβ line was observed together with nearby O I 1027.43 Å, O VI 1037.61 Å, C II 1036.34 and 1037.02 Å lines. Namely 3 large and 14 small scans were performed at the beginning of the run, then almost 1000 and 300 1D exposures were taken in the center of the area using 15 and 2.5 seconds integration times, respectively. The total times of these observational regimes were 25, 22, 232 and 35 minutes.

3. DATA REDUCTION

In order to reduce raw SUMER data the common reduction procedure was applied. After the raw data decompression, the flat-field correction was applied using a revised procedure of T.Kucera. Finally the instrumental spectral line curvature was reduced using the destretching algorithm with the corresponding auxiliary data of T.Moran. All steps of reduction were tested using different data or alternative algorithms with the aim to estimate both possible uncertainties of data and an accuracy of their reduction. The test results consisting of both C II and O VI lines are illustrated below on 75x120 pixel frames.

3.1. Flat-field Reduction

The routinely acquired flat-field data of the SUMER detector A were available from two moments, 13 days before and 4 days after our observations. Although the later one is more close to the actual time of our measurements we have tested the differences of the flat-field information with the aim to estimate the possible uncertainties which could be caused by the long-term changes of the detector sensitivity in different pixels. The appropriate parts of the normalized flat-field frames are displayed in Fig.1 together with their differences. The remarkable differences up to 50% were found for several pixels together with a column pattern of changes in general. Both flat-field frames were used for the reduction of the selected individual spectral frame as well as for the averaged spectral image made from 100 frames of the same position. The normalized differences between the frames reduced using different flat-fields are still of the same order and morphological pattern (see bottom panels of Fig.1, where the results of the individual frame are displayed). This phenomenon can affect of course not only the individual data in spectral line profiles but consequently the inferred spectral line characteristics as well. The illustration of this effect is given in Fig.2, where the maximal intensities and the Doppler line shifts inferred from the selected spectral frame are plotted against the spatial position (slit length). Random fluctuations of these parameters caused by the flat-field data differences can be clearly determined and they are significant particularly in case of the Doppler shifts (e.g. pixel rows 32-35).

The presented inspection of the flat-field information as well as its effect on the spectral characteristics can avoid the instrumentally caused fluctuations from the inferred line parameters. The column-like pattern of the flat-fielded differences could open a possibility to suppress the temporal changes of the flat-field. The imprints of the column like spectral lines could be temporally localized between the moments of its actual measurement using the “history memory” information of the detector if the later will be available with higher temporal resolution.

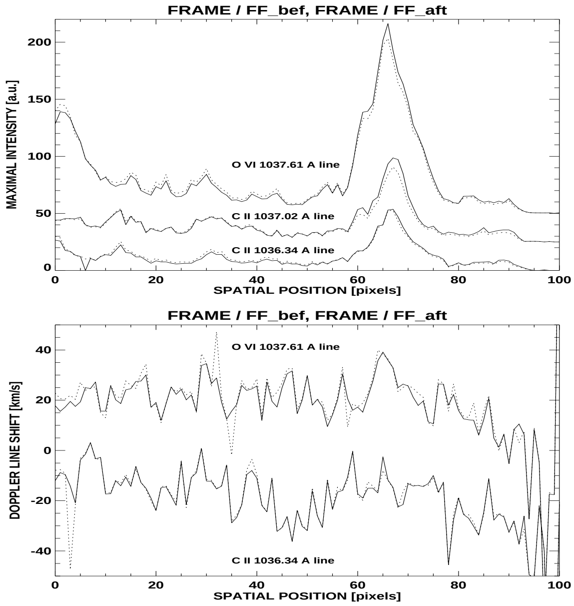

Figure 2. The spatial behaviour of the maximal line intensity and the Doppler shift inferred from one spectral frame applying both pre and past flat-field images is plotted using the solid and dotted lines, respectively. Two upper intensity curves were shifted for 25 and 50 a.u. for better clearness. The Doppler shifts are shifted symmetrically for ±25 km/s from the zero velocity level.

Due to unknown reasons the upper part of the used subarea of the detector (pixel rows 91-120) has not provided significant counts contrary to the rest of it. We were forced to omit this part from analysis.

3.2. Noise Estimation

Noise was found to be above the photon noise statistics as inherent in any SUMER raw image. Therefore an estimation of the instrumental noise can be valuable for each observation. In our case, the last part of measurements - burst sequence of images of short exposures - is appropriate for the determination of the upper limit of this noise. After the examination of these spectral frames and their spectral characteristics, derived from them, a continuous sequence of 100 frames (the total time of 250 seconds) was selected without any significant changes of the investigated parameters which at the first sight could be of the solar origin. Assuming that all changes of these profiles were caused only by the instrumental noise the mean spectral frame (averaged counts in each pixel of frames) and consequently the standard deviations frame from the mean were calculated (see Fig.3). The constructed N/S frame shows that the relative errors caused by noise are dominant outside of the spectral line profiles and decrease with the increasing level of counts going to the spectral line cores (right panel of Fig.3). Therefore we have tried to exclude the more noisy positions in the spectral frames. The spectral line characteristics - the maximal intensity and the Doppler velocity - were determined only from lower number of spectral profile points in the core of the spectral lines without an approximation of the whole spectral line profile. Besides of this, the smoothing of the spectral profiles was applied in the spatial direction in order to decrease noise scatter of data.

The illustration of the determined overestimation of the instrumental noise at individual spectral profiles is given in Fig.4 both for the brighter network boundary and quiet internetwork profiles.

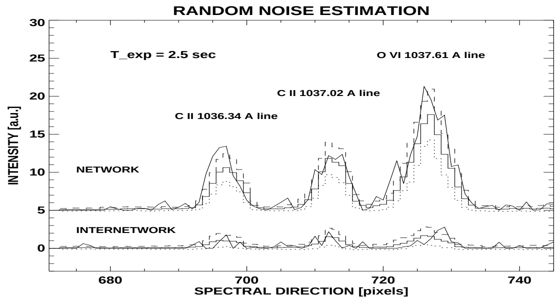

Figure 4. Examples of two spectral profiles of C II and O VI lines representing the supergranular boundary and internetwork are plotted using the mean profile (solid line histogram) as like as the mean with the deviations added and subtracted (dashed and dotted histograms). An example of the individual profiles, from which the statistics were calculated is replotted using the smooth solid line. The artificial shift of the boundary profiles for 5 a.u. was applied.

3.3. Line Destretching

The geometric distortion of the spectral information in the raw SUMER frames has to be destretched in order to straight the spectral lines and remove the instrumentally caused shifts of lines. It would blend the shifts of spectral lines which are intended to be interpreted as the Doppler velocities of the solar origin (Wilhelm et al., 1997). Nevertheless our destretched frames still exhibit significant trends of the spectral line curvatures along the slit which might be at the first sight an instrumental effect (see e.g. the left panel of the Fig.3). Therefore an alternative approach of the distortion correction was tested on the base of the both 2D scan frames taken at the beginning of the observational run. Our assumption that the averaging of the available exposures in different positions on the solar disk will be sufficient to smear out the Doppler velocity fluctuations along the slit has not been confirmed (see Fig.5 for the O VI line results). The averaged intensity profiles from different positions show that at least in the particular case of the present run there exist the correlation of the line emission intensity and Doppler velocity. This caused that the large-scale Doppler velocity pattern is still surviving in all investigated lines for a significant part

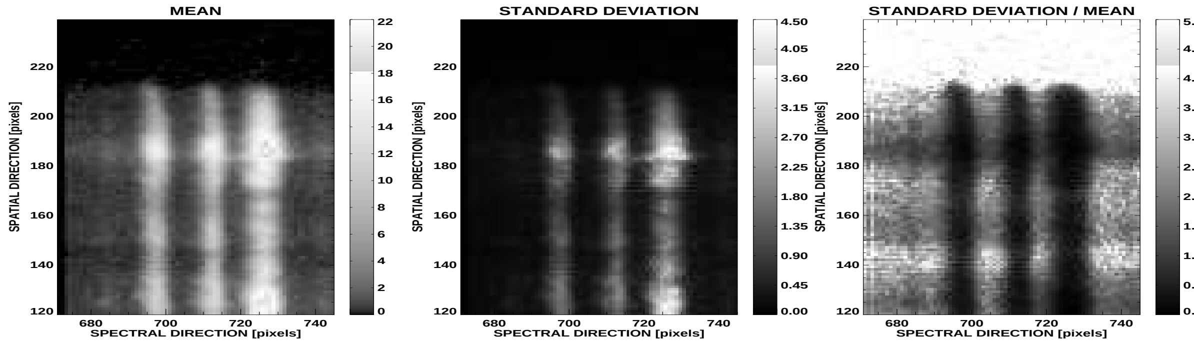

Figure 3. *Panels display the mean spectral frame of 100 similar 2.5 seconds exposures of C II and O VI lines (left), the standard deviations from this mean frame for each pixel (middle) and the normalized N/S (deviation/mean) frame (right).*

of the slit length. Finally we decided to interpret all fluctuations of the spectral line displacements as the Doppler velocities of the emitted solar plasma.

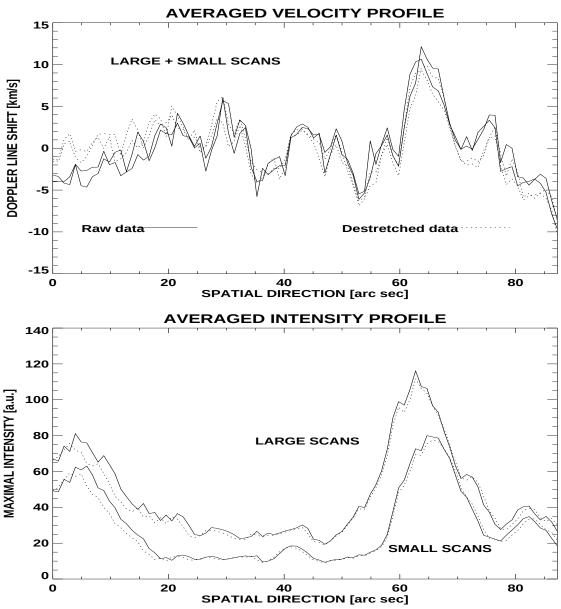

Figure 5. *The plot gives the averaged velocity as well as intensity profiles of the O VI line, derived from both large and small 2D scans. The line displacements in these averaged behaviour show also some large-scale changes which seems to be related to the averaged intensity profiles for the upper part of the slit.*

3.4. Spectral Characteristics Calculation

Calculating the temporal behaviour of the spectral line characteristics from the SUMER reduced frames one has a relative freedom to select the appropriate values of numerical parameters, namely : $\triangle\lambda$, $\triangle$y, $\triangle$t standing here for the spectral, spatial and temporal resolutions respectively. We have tested several combinations of these parameters together with the application of the following limiting conditions and criteria : the zero level of the continuum emission was proposed around the investigated lines; the individual spectral profiles were smoothed using the running mean averages of 5 points; no data binning was applied in the wavelength direction ($\triangle\lambda$=0.0445 Å); the maximal intensity and the Doppler shifts of lines were detected from the second order polynomial approximation of 5 points, selected symetrically around pixel of the maximal intensity from the smoothed line profiles; cases when it was numerically impossible to determine the reliable line shifts were omitted; the Doppler velocities were averaged over the whole domain in order to get a reference zero velocity which was then subtracted from velocity results.

Finally, the combination of the no temporal averaging and spatial summation of 2 adjoining spectral profiles was selected for the calculation of the time-slice maps of the maximal intensity and the line shifts of different lines. The spatial degradation was applied according to the fact that the smallest solar structure determined by the SUMER along the slit was 2 arc sec (Lemaire et al., 1997) and the resulting value of the applied spatial resolution was set to $\triangle$y=1.96 arc sec. This possibility was preferred in order to improve the SNR of the spectral profiles without the decrease of the inferred temporal resolution. Only 16 results were omitted due to numerical reasons over the whole time-spatial domain of SUMER data from 3 lines (two C II and one O VI) acquired with the integration times from 2.5 up to 15 seconds (only 2 of them were from the 1D long-term measurements).

4. RESULTS AND DISCUSSION

The determined time-slice maps of the maximal intensity and the Doppler velocity behaviour of the O VI 1037.61 Å line are reproduced in Fig.6. These results were not smeared additionally for the display purposes to keep the real scatter pattern visible. In the intensity map the column discontinuities reflect the step-like correction of the solar differential rotation which was applied only after each 30 exposures (approx. 8 minutes) shifting the slit for 0.38 arc sec. The velocity time-slice map was originally heavy influenced by the significant long-term periodicities of the overall line displacement with the most likely amplitude of 5 km/s and the period of roughly 2 hours illustrated in Fig.7. This general movement of the spectral image in the direction of the dispersion could be caused by the thermoelastic oscillations of the SUMER mechanics. Although the spectrometer

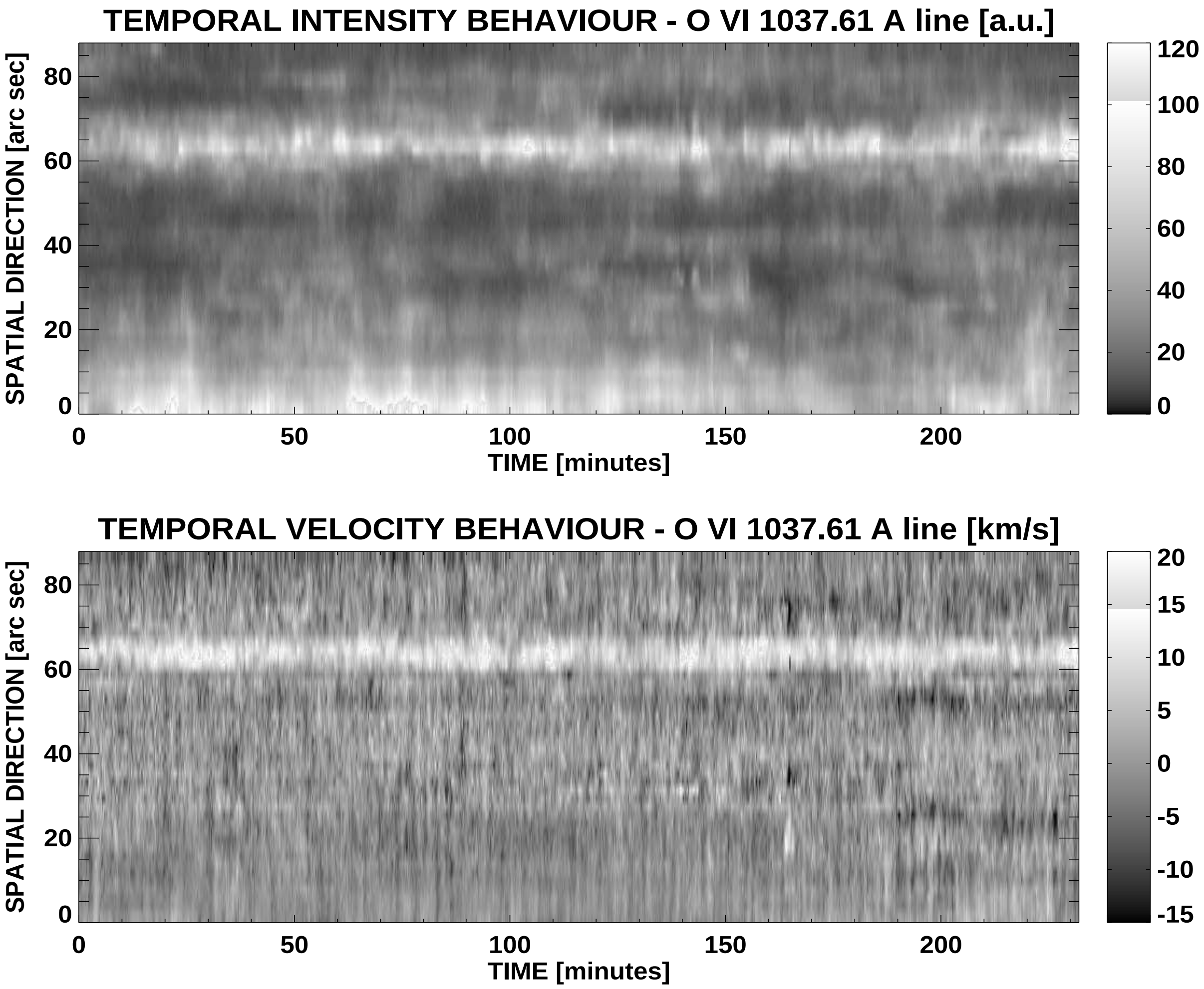

Figure 6. The time-slice maps of the maximal intensity (upper panel) and the Doppler velocity (bottom panel) of the O VI 1037.61 Å line as they were inferred from the 1D long-term measurements with the resolutions of $\triangle y$=1.96 arc sec and $\triangle t$=15 sec.

is thermally controlled, it shows changes by the temperature with the amplitude of 0.15 K. This could be enough at some times to cause just the observed effects. Therefore the log file of the heating control is of the particular interest to authorize whether these overall drifts of spectral images are really caused by the mentioned reason. In order to suppress this instrumental effect the long-term smooth of the spatially averaged velocity pattern was calculated (see Fig.7). This overall line drift was removed respectively from the velocity time-slice map. The velocity map seems to exhibit for the first sight a significant random fluctuations. However the detail inspection of these results has shown that their behaviour is rather smooth and that the impression is caused only by the rather narrow illustration of high number of data. Also some large blue shifts which has appeared in the internetwork are real.

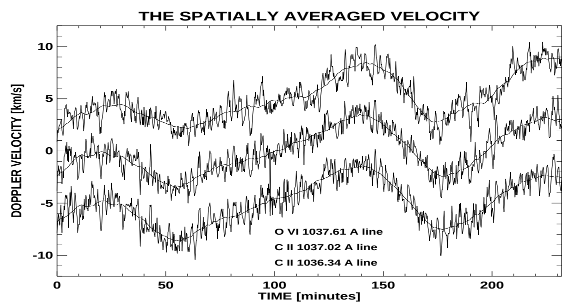

Figure 7. The spatially averaged temporal behaviour of the line displacements are plotted for all 3 lines (C II and O VI) together with the calculated long-term smooth of these data. The artificial shifts for ±5 km/s were applied to distinguish behaviour of these lines.

Generally the time-slice maps of O VI line (Fig.6) show significant spatial differences according to the supergranular network as well as remarkable temporal changes of the presented characteristics. The bright network area is correlated with the systematic red-shift of the O VI transition region line (from 5 to 20 km/s) and the internetwork regions with the velocities centred on zero but with the standard deviation of 3 km/s also in the most dark areas (Fig.8). The similar effect was already presented by Steffens et al. (1997) from the SUMER data. These relation does not seem unambiguous. The more condensed network boundary situated in the upper part of the maps is not the brightest part of the map but its Doppler velocity reaches the highest values. Therefore it is clear that there must be additional conditions required to get the mentioned I-V relation besides of the position on the supergranular boundary. The opposite V-I relation, but of the very small differences, was detected in the C II lines.

The temporal evolution is relatively significant in all C II and O VI lines not only at the supergranular boundary but even in the internetwork areas. They are well above the noise level and therefore their frequency distribution can be studied.

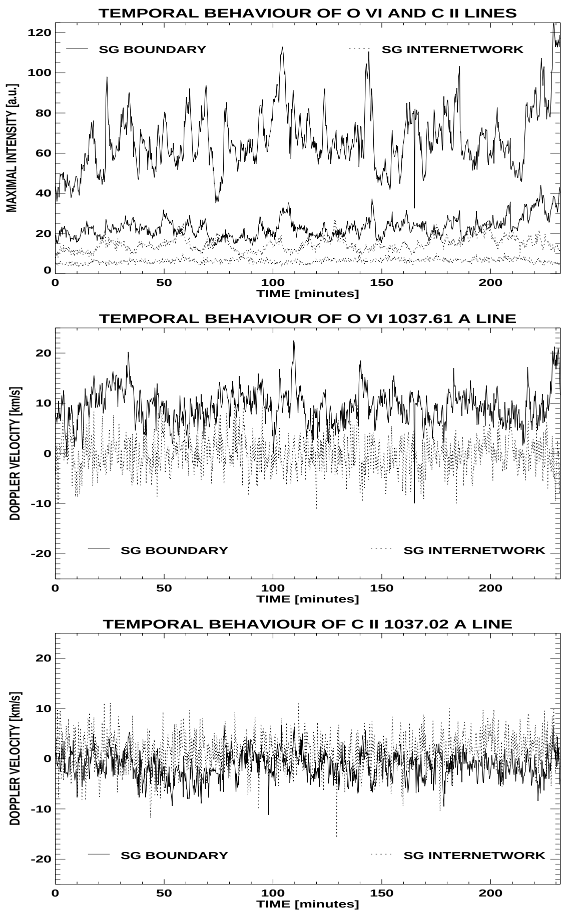

Figure 8. Examples of the maximal intensity (upper panel) and the Doppler velocity (bottom panels) temporal behaviour for the most pronounced network boundary (the spatial position of 63 arc sec in the Fig.6) and the darkest internetwork (the position at 45 arc sec). The O VI and C II lines parameters are displayed.

5. CONCLUSIONS AND OUTLOOK

The tested flat-field and destretching corrections allowed, together with noise estimation, a reduction of SUMER data in the way that the resolution limits of $\triangle\lambda$=0.0445 Å, $\triangle$y=1.96 arc sec and $\triangle$t=15 sec were applied for the construction of the spatial and temporal behaviour of the spectral line characteristics.

The investigated O VI and C II line measurements revealed the significant spatial and temporal fluctuation both in the intensity and the Doppler velocity. The intensity ratio of up to 10 was detected when the most pronounced network intensity was compared to the darkest internetwork. In the network boundary the general O VI line red-shift from 5 to 20 km/s was found, while the internetwork has shown very lower blue-shift relatively to the mean zero velocity level. In case of the C II line this effect was inverted, but of the very small difference. Nevertheless these relations were found to be conditioned also by other physical requirement(s) as the described relationship has been found not unambiguous.

The resulting data were inferred with the precision which will allow more sophisticated and/or more detailed investigation. Beside of this, the Lyβ line will be added to the present O VI and C II lines in order to extend the upper chromosphere diagnostics. The final conclusions would be made only from a larger volume of the observational data after combination with the VTT observations results.

ACKNOWLEDGMENTS

SOHO is a project of international cooperation between ESA and NASA. The SUMER project is financially supported by DARA, CNES, NASA and PRODEX (Swiss contribution). Additional support was provided by the participating institutions. We particularly appreciate the efforts of the SUMER operations team which has help a lot also in case of our project. A.K. and J.R. are grateful to the Slovak grant agency for science (grant No. 2/4154/97) for partial supporting of this work. A.K. thanks for support by the bilateral german-slovak scientific-technical cooperation project X261.1. The presentation of this contribution on 5th SOHO workshop was allowed by kind financial support of the SOC and LOC given to J.R.

REFERENCES

Curdt, W., Kučera,A., Rybák,J., Schühle,U., Wöhl,H., 1997, in *'Advances in the Physics of Sunspots'*, eds. B. Schmieder, J.C. del Toro Iniesta, and M. Vázquez, ASP Conf. Ser., 118, 322

Espagnet, O., Muller, R., Roudier, Th., Mein, N., Mein, P., 1995, A&A Suppl.Ser., 109, 79

Kučera, A., Rybák, J., Wöhl, H., 1995, A&A, 298, 917

Lemaire, P., Wilhelm, K., Curdt, W. et al. 1997, Sol.Phys., 170, 105

Steffens,S. Deubner,F.-L., Fleck,B. et al. 1997, in *'Advances in the Physics of Sunspots'*, eds. B. Schmieder, J.C. del Toro Iniesta, and M. Vázquez, ASP Conf. Ser., 118, 284

Wilhelm, K., Curdt, W., Marsch, E. et al. 1995, Sol.Phys., 162, 189

Wilhelm, K., Lemaire, P., Curdt, W. et al. 1997, Sol.Phys., 170, 75